

Sea Surface Slicks Characterization in SAR Images

T. F. N. Kanaa

*Ecole Nationale Supérieure
Polytechnique (ENSP) de
Yaoundé, B.P. 8390, Yaoundé,
Cameroun. Email :
t_kanaa@yahoo.fr.*

G. Mercier

*Ecole Nationale Supérieure des
Télécommunications (ENST) de
Bretagne, Technopole Brest-
Iroise, 29238 Brest, France.
Email :
[Gregoire.Mercier@enst-
bretagne.fr](mailto:Gregoire.Mercier@enst-bretagne.fr).*

E. Tonye

*Ecole Nationale Supérieure
Polytechnique (ENSP) de
Yaoundé, B.P. 8390, Yaoundé,
Cameroun. Email :
tonyee@hotmail.com.*

Abstract – The authors present a new method to characterise and discriminate oil slicks and some look-alikes in ERS-2 SAR images according only to the observed sea roughness, to reduce oil spill detection and monitoring systems cost. It exploits sea wave spectrum images from the multiscale analysis based on a modified morphological pyramid. Many backscatter characteristics extracted at each level, depended on object and background features are normalized to make its spectral scales be identical. Twenty objects (spot and border) backscatter features have been measured. Eleven sea surface slicks types have been analysed, namely oil, atmospheric instability, wind front, unstable air-mass, current front, falling land wind, large gravity waves, low wind area, natural slicks, swell visible and wind sheltered area. The results presented as smoothed *basic profiles* and *textural spectra* allow to tackle oil slicks supervised classification in new images. *Oil slicks* and *current front* are discriminated. But, some ambiguities of slicks discrimination in SAR images remain persistent.

I. INTRODUCTION

Different investigations has approved of the synthetic aperture radar (SAR) images processing diagram for oil slick detection in three steps [1]: dark spots detection, dark spots features extraction and spots classification. Most of dark spots detection algorithms do not take to account the sea state [2]. The study of the dampening of the wave spectra energy has been done by the multiscale analysis of the remotely sense observation. Wavelets transforms are first used, and a Markov chain model is applied for the slick segmentation [3]. Then a modified morphological pyramid is included to the fuzzy c-mean algorithm for the refinement of the detection results [4].

In general, the detected spot need several information de be classify as oil slick or its look-alikes, particularly the characteristic image expression, the backscatter profiles and gradients, the geographical occurrence and the weather limitations [5]. Unfortunately, this approach costs a lot and results always to an supervised classification. The oil slick detection problem needs information at real time. This has drive some

scientists to consider the geometrical features, a few surroundings synergetic data [6] by making contextual analysis, and the backscatter values [7, 8, 9, 10]. In the actual condition, auxiliary data are expensive and not available. This forces the authors to work with only textural measures of the backscatter values to reduce oil spill detection and monitoring systems cost.

Oil slick floating on the sea surface has an influence on these ocean properties [11]. The physico-chemical results of the hydrophobic interaction between the water and the oil involve the mutual dissolution of the one in the other. This mixture gives place to three layers according to the intensity of the mixture agitation : floating oil, layer of conflict and sea water not polluted. The layer of conflict, located at the intermediary of both others, is called the mixture saturated solution or dispersed phase. It creates much confusion in the images and is characterized by a dynamic mixture of the two fluids. According to this hypothesis, all three corresponding regions in the sea SAR image named as spot, border and background remain interesting for slicks characterization.

The multiscale approach is set about dark spot detection and objects features extraction (§II). The data used and the textural profiles obtained are then presented (§III), slicks discrimination is experimented in three new images with contents not identified (§IV), the comments and the futures improvements are described in §V.

II. CHARACTERIZATION METHOD

A. Dark spot detection

This multiscale analysis is carried out by the use of a modified morphological pyramids on adaptive filtering [4]:

$$f_{FI}^{j+1} = E(f_{FI}^j) + [f_{FI}^j - E(f_{FI}^j)] \cdot e^{-\frac{cv_{GC}^j \cdot f_{GC}^j}{\sqrt{f_{GC}^j - f_{GC}^j}}} \quad (2.1)$$

Where f_{FI}^0 represents the original SAR image, f_{FI}^j is the filtering image on level j , $E(\circ)$ the mean of image \circ , $\vee f_{GC}^j$ the maximum value of the gradient contrast image at level j named f_{GC}^j , cv_{GC}^j the latter coefficient of variation. The multi-resolution non linear decomposition generates wave spectrum (WS) images f_{WS}^j ($j=1,2,3,\dots$), representative of the informational contents of the sea wave spectrum. The detection of the tasks is then made by the centralized fuzzy data fusion of WS images and the maximum of the membership rule.

B. Objects features extraction

Geometrical features are first measured: area A , perimeter P and complexity C [8]. Then, the slick regions are directly analyse in the WS images, at each level j . The features designed by “ λ ” are measured and renamed as the *object- λ -ratio* ($O\lambda R$) presented as comparative value $\eta_{O\lambda R}(j)$ (2.2).

$$\eta_{O\lambda R}(j) = \frac{1000 \cdot \lambda_{object}^j}{\lambda_{object}^j + \lambda_{back}^j} \quad (2.2)$$

Where λ_{object}^j and λ_{back}^j are respectively the object and background features respectively corresponding. The followings features for which some one stem from [7] and [8] are measured for the spots, the borders and the backgrounds corresponding : dynamic ratio d_{Object}^j (2.3), contrast c_{Object}^j as the mean of the WS image contrast f_C^j (2.4), mean μ_{Object}^j , standard deviation σ_{Object}^j , power to mean ratio $\sigma_{Object}^j / \mu_{Object}^j$, gradient dynamic ratio, gradient contrast, gradient mean, gradient standard deviation, gradient power to mean.

$$d_{Object}^j = \frac{\vee_{Object} f_{WS}^j - \wedge_{Object} f_{WS}^j}{\vee_{Object} f_{WS}^j} \quad (2.3)$$

$$f_C^j = \frac{1}{k^2 - 1} \sum_{s_q \in D_k^i} |f_{WS}^j(s_i) - f_{WS}^j(s_q)| \quad (2.4)$$

Where D_k^i is the 8-connexity neighbor ($k=3$) of the common pixel s_i , $\vee_{Object} f_{WS}^j$ ($\wedge_{Object} f_{WS}^j$) the object maximum (minimum) value on f_{WS}^j . The textural features “ $O\lambda R$ ” are then called SdR (Spot dynamic Ratio), ScR (S. contrast R.), SmR (S. mean R.), SsdR (S. standard deviation R.), SpmR (S. power to mean R.), SgdR (S. gradient d. R.),

BdR (Border d. R.), ... The results obtained of the characterization of WS images are presented first in one dimensional (1-D) smoothed profiles form $\eta_{O\lambda R}(j)$ (in ‰), then in 2-D profiles form $\eta_{O\lambda R}(j, O\lambda R)$ (in ‰) named as the textural spectra (3-D graphs top view) of the sea surface slicks. The basic profiles can be draw by using the truth ground images with different slicks contents. Any similar signature would then refer to them for a possible discrimination.

III. DATA AND RESULTS

A. Data

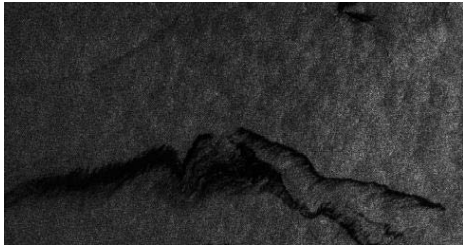
To draw the basic profiles, a bank of eleven SAR images of the ERS-2 satellite (Fig. 1), acquired for the monitoring of the Mediterranean sea on 1999 and 2000, are available. The following slicks of oil and other atmospheric and oceanic phenomena origin would be characterised.

1. *Oil slicks* SAR image (486×256) with old slicks modified by current and by wind (Fig. 1a, folio 1), date 4/12/99, location MALTA.
2. *Atmospheric instability* SAR image (400×400), date 8/11/99, location EGYPT (Fig. 1b, folio 1).
3. *Wind front* SAR image (400×400), date 17/12/99, location MALTA.
4. *Unstable air-mass* SAR image (400×400), date 20/01/00, location CORSICA.
5. *Current front* image (400×400), date 17/01/00, location GIGLIO ISLAND (Fig. 1c, folio 1).
6. *Falling land wind* SAR image (400×400), date 30/11/99, location ADRIATIC.
7. *Large gravity waves* with not apparent rain cells, Medium wind conditions, SAR image (400×400), date 18/04/00, location EGYPT.
8. *Low wind area* SAR image (400×400), date 4/12/99, location BALEARI.
9. *Natural slicks* in current vortices, SAR image (400×400), date 5/02/00, location EAST of CORSICA (Fig. 1d, folio 1).
10. *Swell well visible* in SAR image (400×400), date 4/12/99, location BALEARI (Fig. 1e, folio 2).
11. *Wind sheltered area* SAR image (256×256), date 27/11/99, location MOROCCO.

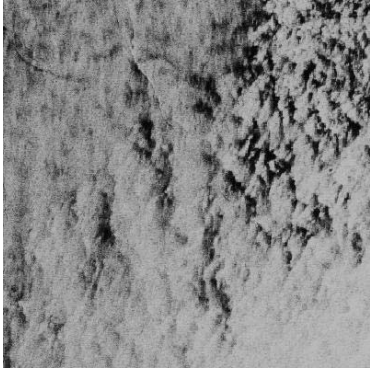
Three other images located in DOUALA, with slicks not identified will be used: ERS-2 SAR image *Unknown slicks 3*, size 270×270, date 17/11/99, (Fig. 1f, folio 1); ENVISAT ASAR images *Unknown slicks 2* (Fig. 1g, folio 2) and *Unknown slicks 1* (Fig. 1h, folio 2), size 400×400, acquired on 2003.

B. Results

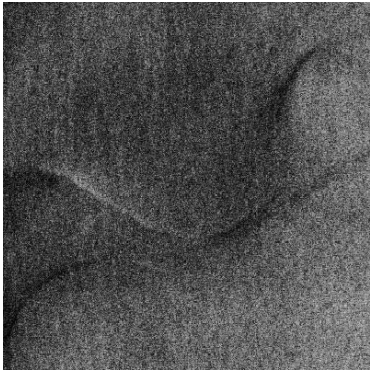
Eleven sea surface slicks have been analysed, namely oil, atmospheric instability, wind front, unstable air-mass, current front, falling land wind, large gravity waves, low wind area, natural slicks, swell visible and wind sheltered area.



(a)



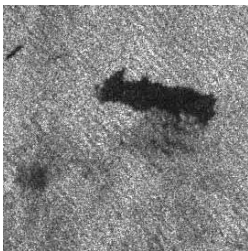
(b)



(c)

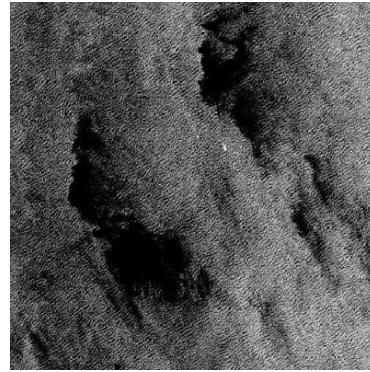


(d)

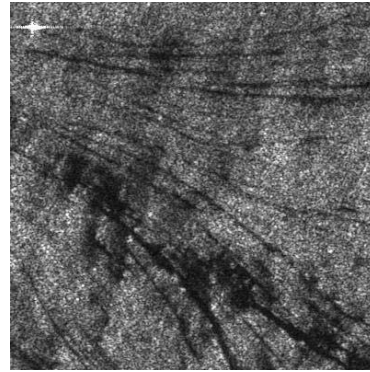


(f)

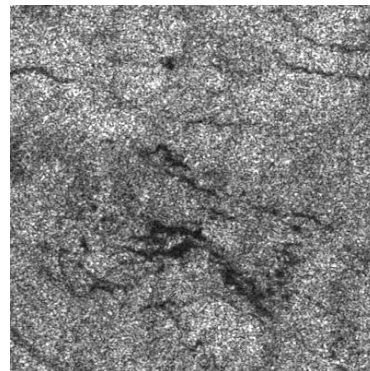
(Fig. 1, folio 1)



(e)



(g)



(h)

(Fig. 1, folio 2)

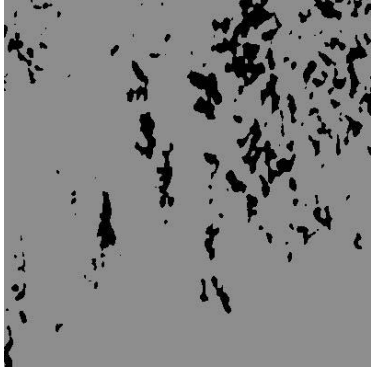
Fig. 1. Original truth ground SAR images and original unknown slicks images of the ERS-2 and ENVISAT satellites. © ESA (European Space Agency)

Folio 1: (a) Oil slicks, (b) Atmospheric instability, (c) Current front, (d) Natural slicks, (f) Unknown slicks 3.
Folio 2: (e) Swell, (g) Unknown slicks 2, (h) Unknown slicks 1.

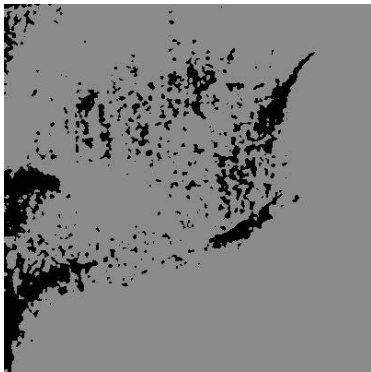
For these results, five truth ground data and three unknown slicks images are selected for the simulation (Fig. 1). The spots are first detected (Fig. 2). Its geometrical features, in particular area A , perimeter P and complexity C , are measured and visible in the latter figure. Then, the slicks smoothed profiles $\eta_{O\lambda R}(j)$ are constructed for each feature $O\lambda R$ depending on the scale j . Only four examples (SmR, SpmR, SgcR, BdR, BgdR, BgpmR) are presented in Fig. 3. The 3-D graphs top view $\eta_{O\lambda R}(j, O\lambda R)$ corresponding are drawn too in Fig. 4.



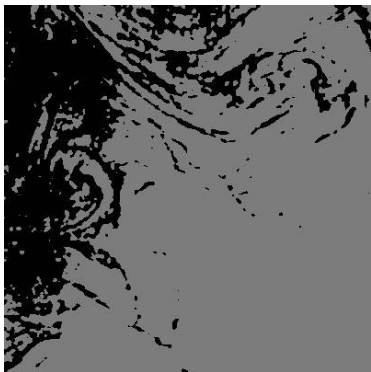
(a)



(b)



(c)

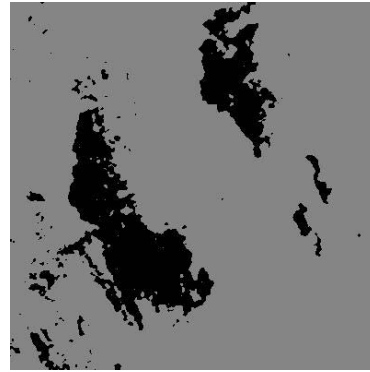


(d)

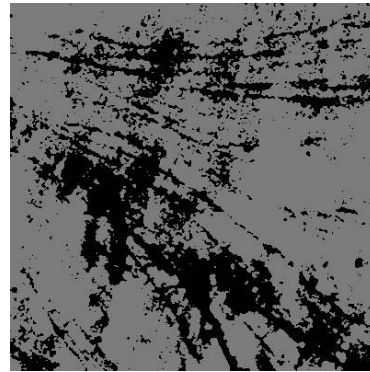


(f)

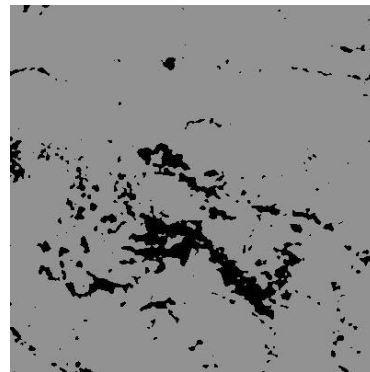
(Fig. 2, folio 1)



(e)



(g)



(h)

(Fig. 2, folio 2)

Fig. 2. Spot detected in Original truth ground SAR images and original unknown slicks images of the ERS-2 and ENVISAT satellites, with following geometrical features (px: pixels).

Folio 1:

(a) Oil slicks, $A = 13155$ px, $P = 2012$ px, $C = 4.95$;

(b) Atmospheric instability, $A = 16365$ px, $P = 6343$ px, $C = 13.1$;

(c) Current front, $A = 17592$ px, $P = 8447$ px, $C = 17.97$;

(d) Natural slicks, $A = 43178$ px, $P = 9880$ px, $C = 13.42$;

(f) Unknown slicks 3, $A = 6358$ px, $P = 1092$ px, $C = 3.86$;

Folio 2:

(e) Swell, $A = 24040$ px, $P = 4660$ px, $C = 8.48$;

(g) Unknown slicks 2, $A = 46043$ px, $P = 21708$ px, $C = 28.54$;

(h) Unknown slicks, $A = 13631$ px, $P = 6634$ px, $C = 16.03$.

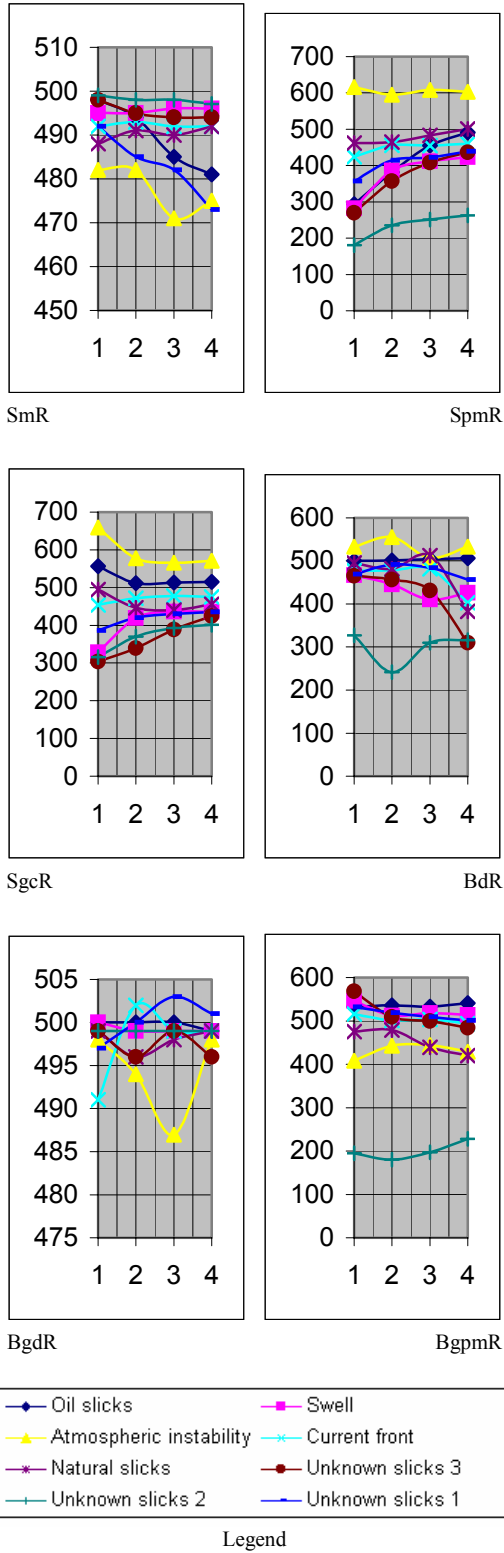


Fig. 3. 1-D smoothed profiles $\eta_{O\lambda R}(j)$ (in $\%$, function of scale j) for five truth ground data and three unknown slicks images.

IV. SLICKS DISCRIMINATION

The slicks discrimination principle is the supervised comparison of its textural profiles, in particular its textural spectra.

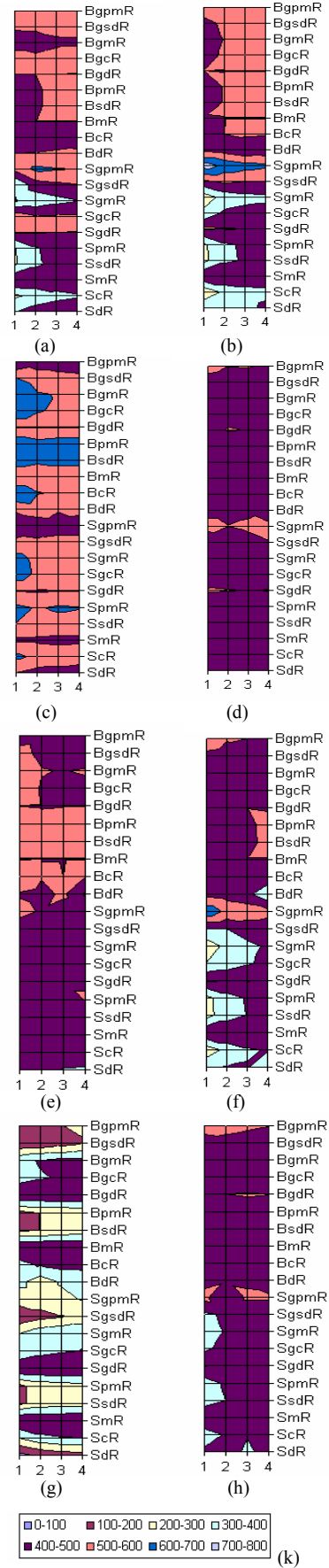


Fig. 4. Textural spectra (2-D profiles) $\eta_{O\lambda R}(j, O\lambda R)$ (in $\%$, function of scale j and feature $O\lambda R$),

for five truth ground data and three unknown slicks images. The colours correspond to the legend values bands.

(a) Oil slicks, (b) Swell, (c) Atmospheric instability, (d) Current front, (e) Natural slicks, (f) Unknown slicks 3, (g) Unknown slicks 2, (h) Unknown slicks 1, (k) Legend.

The colours corresponding to the values bands make the analysis easier. The basic profiles drawn with the truth ground data are the models. The unknown slicks are similar signatures that refer to them for a possible discrimination. The profiles obtained on these new three images are compared with the basic profiles.

The unknown slick 3 textural spectrum (fig. 4f) looks alike oil (fig. 4a) and swell (fig. 4b) slicks spectra. But it is more similar to the first. Therefore, the dark detected corresponding is classified as oil slick. The unknown slick 2 textural spectrum (fig. 4g) is difficult to analyse. It highlights the usual ambiguities which come up in the slicks discrimination. The unknown slick 1 textural spectrum (fig. 4h) looks alike current front spectrum (fig. 4d). The spot is then considered as oil slick look-alike, in particular as current front. But seemingly, it isn't the latter, it would be another kind of slick looking like current front.

V. CONCLUSION

A method to characterise sea surface slicks in SAR images for its supervised discrimination has been proposed. It has been based on the multiscale image decomposition provided by a modified morphological pyramid. The method has been applied to ERS-2 SAR images to draw basic profiles. Eleven sea surface slicks have been analysed, each of them has provided a nearly unique textural spectrum in spite of the varying context and the presence of the speckle noise. The tests have been carried out in three ASAR images of ENVISAT satellite with contents not identified. One of the unknown slicks has been classified as oil slick, one as possible current front, and the third has presented a failure test, certainly because of its large complexity.

The present experiment results encourage to deal with the correlation measure of the unknown slicks compared with basic profiles for slick regions discrimination in sea SAR or ASAR imagery. In the immediate future, it then becomes possible to consider the automatic classification of the detected signatures at lower cost. It would also be necessary to test the proposed method on a very large bank of data equipped with all the slicks already identified on the sea surface for a best validation of this work.

Acknowledgment

The authors would like to thank J. Lichtenegger and the European Space Agency (ESA) for providing the SAR images.

References

- [1] A. H. S. Solberg, F. Albrechtsen, G. Storvik. *Algorithms for Automatic Detection of Oil Spills in SAR images (ADOS)*. Project description, University of Oslo, 8 p., 2002.
- [2] Thomas F. N. Kanaa, E. Tonye, G. Mercier, V. de P. Onana, J. N. Mvogo, P. L. Frison, J. P. Rudant, R. Garello. *Detection of Oil Slick Signatures in SAR Images by Fusion of Hysteresis Thresholding Responses*. IEEE International Geoscience and Remote Sensing Symposium, IGARSS '03 Proceedings, 21 – 25 July 2003, France, Toulouse, vol. 4, p. 2750 – 2752, 2003.
- [3] G. Mercier, S. Derrode, W. Pieczynski, J. M. Le Caillec, and R. Garello, *Multiscale Oil Slick Segmentation with Markov Chain Model*, IEEE International Geoscience and Remote Sensing Symposium, IGARSS '03 Proceedings, 21 – 25 July 2003, France, IEEE 2003 International, Toulouse, vol. 6, p. 3501 – 3503, 2003.
- [4] Thomas F. N. Kanaa, E. Tonye, G. Mercier, V. de P. Onana, J. P. Rudant. *Multiscale Segmentation of Oil Slick in SAR Images based on Morphological Pyramid*. ENVISAT/ERS Symposium Proceedings, 6 – 10 sept 2004, Salzburg, Australie.
- [5] H. A. Espedal. *Oil Spills and its Look-alikes in ERS SAR Imagery*. Earth Observation and Remote Sensing, Russian Academy of Science, n° 5, 1998.
- [6] F. Girard-Ardhuin, F. Collard, G. Mercier, R. Garello. *Oil Slick Classification by SAR Imagery using Synergetic data*. USA Baltic Symposium, Klaipeda, Lithuania, 6 pp, 15-17 June 2004.
- [7] A. H. S. Solberg, G. Storvik, R. Solberg and E. Volden. *Automatic Detection of Oil Spills in ERS SAR Images*. IEEE Transactions on Geoscience and Remote Sensing, vol. 37, p. 1916 – 1924, 1999.
- [8] Fabio Del Frate, A. Petrocchi, J. Lichtenegger, G. Calabresi. *Neural Networks for the Oil Spill Detection using ERS-SAR Data*. IEEE Transactions on Geoscience and Remote Sensing, vol. 38, p. 2282 - 2287, 2000.
- [9] K. W. Bjerde, A. H. S. Solberg and R. Solberg. *Oil spill detection in SAR imagery*. IEEE International Geoscience and Remote Sensing Symposium, IGARSS '93 Proceedings, vol. 3, p. 943–945, 1993.
- [10] G. Benelli, A. Garzelli. *Oil-Spills Detection in SAR Images by Fractal Dimension Estimation*. IEEE International Geoscience and Remote Sensing Symposium, IGARSS '99 Proceedings, 28 June-2 July 1999, Hamburg, Germany, vol. 1, p. 218 – 220, 1999.
- [11] Thomas F. N. Kanaa, E. Tonye, G. Mercier, V. Onana. *Détection des Nappes d'Hydrocarbures dans les Images RSO par Morphologie Mathématique*. Télédétection, vol. 4, n° 3, p. 215 – 229, 2004.